JPE 19-2-19

https://doi.org/10.6113/JPE.2019.19.2.540
ISSN(Print): 1598-2092 / ISSN(Online): 2093-4718

# Electromagnetic and Vibration Analysis of E-core Switched Reluctance Motor with Permanent Magnets and Auxiliary Windings

Saranya S.† and Balaji M.*

†,*Department of Electrical and Electronics Engineering, SSN College of Engineering, Kalavakkam, India

**Abstract**

In this work a new configuration of E-core stator Switched Reluctance Motor (SRM) with permanent magnets and auxiliary windings embedded in the stator yoke is proposed. For the proposed configuration of SRM electromagnetic analysis is performed using Finite Element Analysis (FEA) based computer aided design package MagNet and to emphasize its merits a comparison is drawn with existing hybrid excitation configuration of SRM. In addition, the vibration characteristics of the motor are analyzed by performing modal and transient analysis using the ANSYS package. Results of the analysis reveals that the proposed configuration of SRM exhibits better electromagnetic and vibration characteristics and is capable of competing with the existing topologies in the variable speed market.

**Key words:** E-core stator, Finite element analysis, Hybrid excitation, Switched reluctance motor, Vibration analysis

## I. INTRODUCTION

Switched Reluctance Motor (SRM) is widely preferred for variable speed applications because of its inherent characteristics like robust construction, high speed, high starting torque and increased fault tolerance [1]-[3]. Various configurations of permanent magnet assisted SRM drives have been proposed with the objective of improving the efficiency and torque density combined with lower cost in order to compete with Brushless DC Motor and permanent magnet synchronous motor drives [8]-[10].

A doubly salient permanent magnet motor with improved torque and efficiency characteristics has been proposed by Yuefeng Liao et al. [4] but this configuration suffers from high torque pulsations. A novel C core stator SRM with enhanced power and efficiency has been proposed by Shang Hsun et. al [5]. In [6] the authors have presented a two phase SRM with flux reversal free stator, that is conceived for high efficiency and full load starting performance. However, due to its asymmetric torque characteristics it cannot be used for four quadrant operation.

A two phase SRM with an E-core stator has been proposed by Cheewoo Lee et al. [7] with the aim of producing shorter flux paths, which leads to reduced copper and core losses. Tae Heoung Kim [8] proposed a flux reversal machine that has permanent magnet embedded parallel to the stator magnetic flux lines to avoid demagnetization problem. In [9] Kaiyaun Lu et al. has presented a single phase hybrid switched reluctance motor, which has ferrite magnets arranged in a special flux concentration manner with the objective of improving torque density and efficiency. A switched reluctance motor with auxiliary windings and permanent magnet has been proposed by Yu Hasegawa et al. [10]. The main advantages of this configuration are its improved average torque and its ability to work in generator mode.

In [11] an improved 9/12 two phase E-core switched reluctance machine has been analyzed. A comparison is drawn with 6/10 configuration to highlight the improvement in average torque and torque density. Di Wu et al. [12] has highlighted the merits of a novel doubly salient synchronous machine with permanent magnets in stator yoke with respect to variable reluctance in terms of torque density and efficiency. The performance of flux reversal machines with inset

Manuscript received Apr. 25, 2018; accepted Nov. 30, 2018
Recommended for publication by Associate Editor Byungtaek Kim.
†Corresponding Author: saranyas@ssn.edu.in
Tel: +91 11 27469700, Fax: +91 44 27469772, SSN College of Eng.
*Dept. of Electr. and Electron. Eng., SSN College of Eng., India

permanent magnets has been discussed by Liang Xu et al. [13]. The main advantage of this configuration is its variable flux capability.

The authors of [14] have proposed a switched reluctance motor with segmented rotor to enhance its performance. In [15] Wei Hua et al. has presented a hybrid excited flux switching machine with an E-core stator which has improved flux regulation capability and extended range of speed regulation. ZihCing You et al. [16] has proposed a novel DC excited flux switching machine which has two layer rotor structure with improved starting torque capability but the amount of torque produced is 13% less than the conventional configuration of SRM. A flux switching machine with permanent magnets embedded in rotor has been presented in [17]. The merit of this configuration includes improved average torque and reduced torque ripple.

Thus, from the analysis of literature it is evident that there is adequate scope for performance augmentation of SRM by introducing permanent magnets in the stator. It is in this perspective a novel configuration of hybrid excited SRM with an E-core stator has been proposed. A comparison is drawn with an existing doubly salient permanent magnet SRM (DSPM SRM) and conventional SRM with hybrid excitation (Hybrid SRM) with respect to electromagnetic and vibration characteristics to highlight the merits of the proposed configuration.

## II. Electromagnetic Analysis of E-core SRM with Permanent Magnets and Auxiliary Windings

The structure of proposed E-core SRM with permanent magnets (PM) and auxiliary windings (AW) embedded in stator yoke (hybrid E-core SRM) is shown in Fig. 1. This hybrid E-core SRM is a two phase motor with four stator main poles and four rotor poles. It has two E-cores, and each of the core comprises three stator poles in which the middle pole is identified as shared pole with two adjacent excitation poles [18]. Each phase comprises of two excitation poles one from each core with concentrated windings around them. Auxiliary windings which are energized by a constant DC current source are wound around the stator yoke. In addition, two permanent magnets are also embedded in the stator yoke as shown in Fig. 1. The flux path at aligned and unaligned position when energizing phase A and phase B are shown in Fig. 2 and Fig. 3. The permanent magnet does not suffer from any demagnetization problem, since the coils of both excitation phases are wound in such a way that they generate flux in the same direction as that of permanent magnet flux.

In this proposed configuration of SRM, when the unaligned phase is excited, less than one third of the stator pole flux traverses the aligned stator and the flux through the shared pole is unidirectional regardless of which phase is excited. These

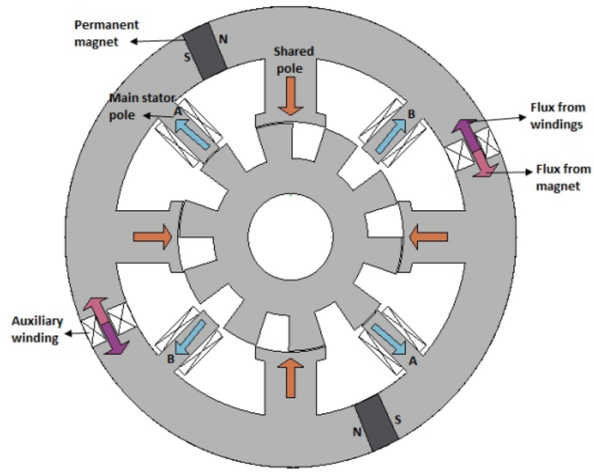


Fig. 1. Structure of hybrid E-core SRM.

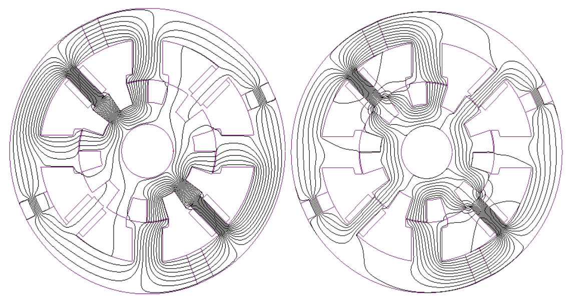

(a) (b)

Fig. 2. Flux lines of hybrid E-core SRM when phase A windings are energized. (a) Aligned position. (b) Unaligned position.

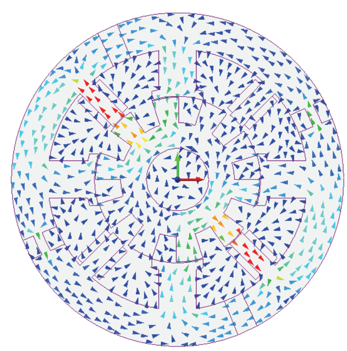

(a)

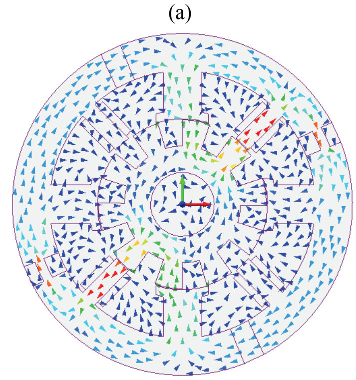

(b)

Fig. 3. Arrow plot for flux distribution of hybrid E-core SRM at aligned position. (a) Phase A energized. (b) Phase B energized.

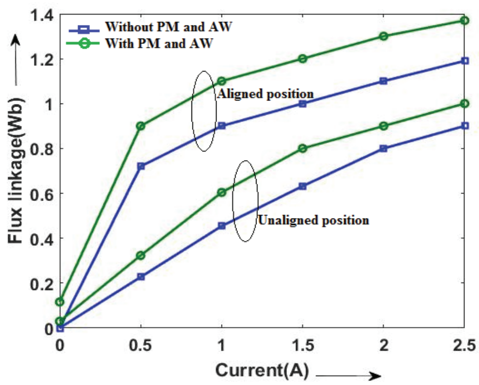


Fig. 4. Static flux linkage vs current characteristics for hybrid E-core SRM with and without PM and AW.

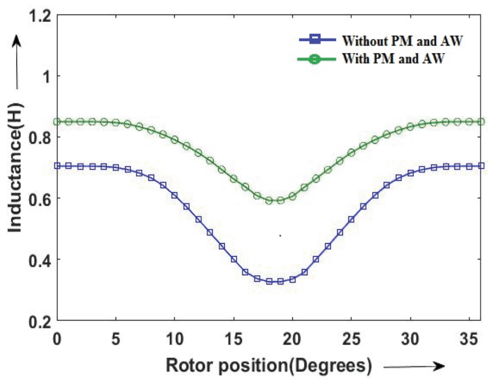


Fig. 5. Inductance profile for hybrid E-core SRM with and without PM and AW.

facts indicate that the stator is free from flux reversals, which is evident from Fig. 2(a) and Fig. 3(a).

For SRM the area enclosed by the flux linkage versus current characteristics indicates the amount of energy converted into mechanical work. Fig. 4 shows the flux linkage vs current characteristics at the aligned and unaligned positions for hybrid E-core SRM with and without permanent magnets and auxiliary windings obtained from FEA analysis under the condition of same ampere-turns. It is evident from this figure that the enclosed area of flux linkage is higher for the proposed configuration of SRM.

Fig. 5 shows the inductance profile of hybrid E-core SRM with and without PM and AW for current level of 1.5A. The improved inductance profile depicted in Fig.5 signifies that the insertion of permanent magnets and auxiliary windings increases the torque production capability. The stroke angle is the angle between the aligned and unaligned positions of rotor for one phase and it is obtained from [19].

$$\theta = (180/N_r) \tag{1}$$

Where, $\theta$ is the stroke angle and $N_r$ is the number of rotor poles. For the proposed configuration of SRM stroke angle is $18^0$ as evident from Fig. 5.

Table I shows the percentage difference in average torque ($T_{avg}$) due to the insertion of PM and AW in the stator yoke for

TABLE I
COMPARISON OF AVERAGE TORQUE

| Current (A) | 0.5 | 1 | 1.5 | 2 | 2.5 |
|---|---|---|---|---|---|
| $T_{avg}$ with PM and AW (Nm) | 0.480 | 1.302 | 1.851 | 2.382 | 2.655 |
| $T_{avg}$ without PM and AW (Nm) | 0.395 | 1.024 | 1.432 | 1.82 | 2.436 |
| % difference | 17.7 | 21.3 | 22.6 | 23.5 | 23.9 |

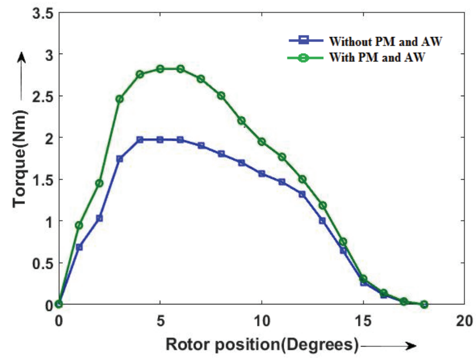


Fig. 6. Torque profile for hybrid E-core SRM with and without PM and AW.

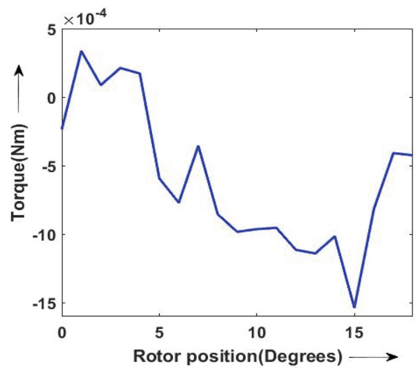


Fig. 7. Cogging torque profile for hybrid E-core SRM.

hybrid E-core SRM. From Table I it is clear that there is significant improvement in average torque due to the insertion of permanent magnets and auxiliary windings. The general expression for average torque in switched reluctance motor when energizing one phase is [20].

$$T_{avg}=(\delta W_m N_s N_r)/4\pi \tag{2}$$

Where $N_s$ is the number of stator poles and $\delta W_m$ is the area between the aligned and unaligned position curves in the flux linkage vs current characteristics.

The static torque profile of hybrid E-core SRM with and without PM and AW for current level of 1.5A obtained from FEA is shown in Fig. 6. It is signified from Fig. 6 that there is a significant improvement in average torque due to the insertion of permanent magnet and auxiliary winding. In addition to electromagnetic torque, cogging torque is also a prime objective, when designing permanent magnet motors. The cogging torque characteristic for the proposed configuration of SRM is shown in Fig. 7. It is clear from Fig. 7 that the hybrid

TABLE II
STRUCTURAL PARAMETERS FOR THREE DIFFERENT CONFIGURATIONS OF SRM

| Parameters | Hybrid SRM | DSPM SRM | Hybrid E-core SRM |
|---|---|---|---|
| No. of stator main poles | 12 | 4 | 4 |
| No. of shared poles | -- | 4 | 4 |
| No. of rotor poles | 8 | 10 | 10 |
| Width of shared pole | -- | 10mm | 10mm |
| Shaft diameter | 20 mm | 20 mm | 20 mm |
| Rotor pole root diameter | 36.4 mm | 36.4 mm | 36.4 mm |
| Rotor crown diameter | 52.6 mm | 52.6 mm | 52.6 mm |
| Stator pole root diameter | 83.2 mm | 83.2 mm | 83.2 mm |
| Stator outside diameter | 113.2 mm | 113.2 mm | 113.2 mm |
| Air gap length | 0.3 mm | 0.3 mm | 0.3 mm |
| Stack length | 60 mm | 60 mm | 60 mm |
| Rated current | 1.5 A | 1.5 A | 1.5 A |
| Rated voltage | 500V | 500V | 500V |
| Rated speed | 2800 rpm | 2800 rpm | 2800 rpm |
| Permanent magnet material | Ferrite | NdFeB | Ferrite |

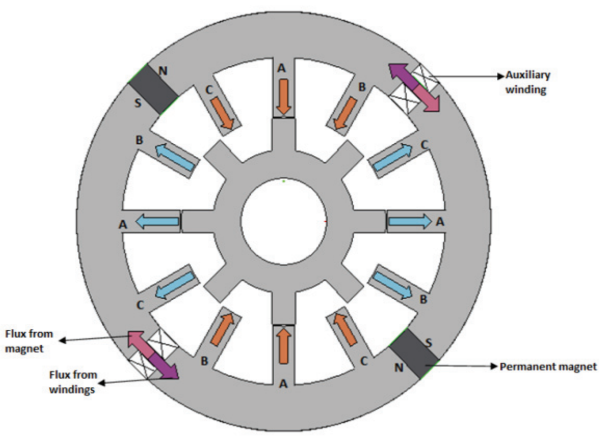


Fig. 8. Structure of hybrid SRM.

E-core SRM has very low value of cogging torque.

## III. PERFORMANCE COMPARISON

With the intention of highlighting the merits of proposed hybrid E-core configuration of SRM in comparison with existing hybrid excitation configuration of SRM, a thorough analysis is carried out by utilizing the FEA based package MagNet and the results are presented. The main dimensions and specifications for all the three configurations of SRM are given in Table II. For a fair comparison certain parameters like stack length, air gap and stator outer diameter are taken same for all three configurations as given in Table II. Fig. 8 shows the structure of hybrid SRM with permanent magnets and auxiliary windings embedded in stator yoke [10]. It has 12 stator poles and 8 rotor poles. For hybrid SRM shown in Fig. 8 the auxiliary windings are energized by a constant dc current source. Fig. 9(a) and 9(b) shows the flux distribution for aligned position of rotor when energizing phase A and phase B. From Fig. 9 it is evident that when the stator pole and back iron section of a phase is completely aligned with the rotor pole it will experience flux reversal by exciting the opposite phase. Hence the stator and rotor iron has bipolar flux and it is not free from flux reversal.

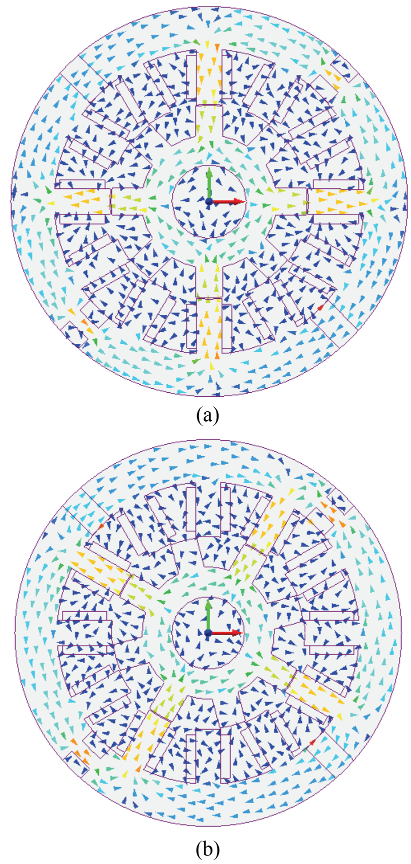


Fig. 9. Flux distribution of hybrid SRM at aligned position. (a) Phase A energized. (b) Phase B energized.

The structure of doubly salient permanent magnet (DSPM) SRM is shown in Fig. 10 [21]. For the DSPM SRM permanent magnets are embedded in common stator poles as shown in Fig. 10. The arrow plot of flux distribution for aligned position of the rotor when exciting phase A and phase B for DSPM SRM is shown in Fig. 11 (a) and 11 (b). It is clear from Fig. 11 that this DSPM SRM has a unidirectional flux through the shared pole and the stator is free from flux reversal which reduces eddy current and hysteresis losses. Due to the presence of permanent magnet cogging torque is introduced in this configuration of SRM. In Fig. 12 the flux linkage characteristics of Hybrid E-core SRM, DSPM SRM and Hybrid SRM are presented under similar rated torque condition. From Fig. 12 it is apparent that the enclosed area of flux linkage for hybrid E-core SRM is superior to DSPM SRM and hybrid SRM at a

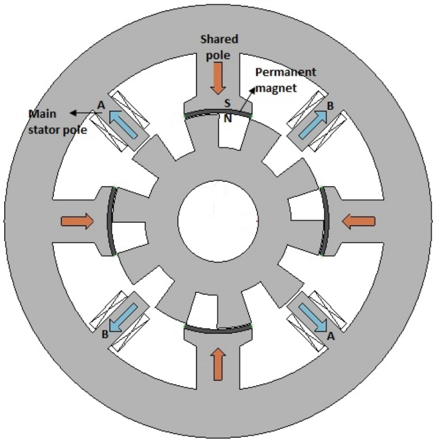


Fig. 10. Structure of DSPM SRM.

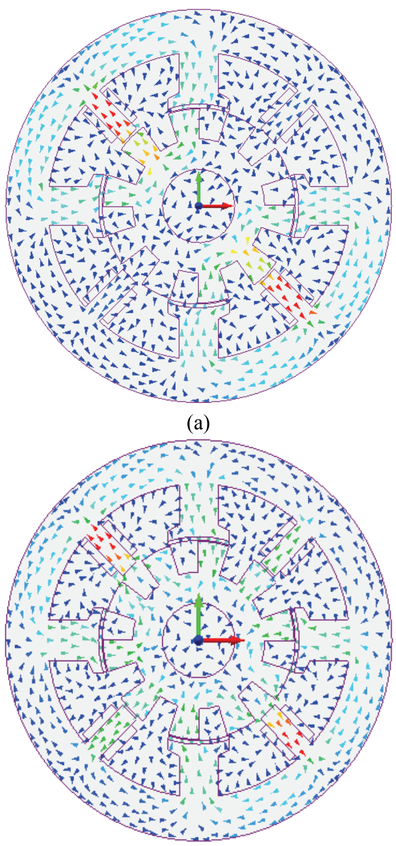

(a)

(b)

Fig. 11. Flux distribution of DSPM SRM at aligned position. (a) Phase A energized. (b) Phase B energized.

fixed current from aligned to unaligned position which infers that the average torque of hybrid E-core SRM is higher than DSPM SRM and hybrid SRM.

In Table III a comparison is drawn between the average torque value of hybrid E-core SRM and the other two existing configurations of SRM. It is obvious from Table III that the hybrid E-core SRM has higher value of average torque than DSPM SRM and hybrid SRM, especially, among large current range and the dominance increases with increase in current.

TABLE III
COMPARISON OF STATIC AVERAGE TORQUES FOR DIFFERENT CURRENT LEVELS

| Current (A) | 0.5 | 1 | 1.5 | 2 | 2.5 |
|---|---|---|---|---|---|
| $T_{avg}$ for Hybrid SRM (Nm) | 0.268 | 0.836 | 1.400 | 2.244 | 2.483 |
| $T_{avg}$ for DSPM SRM (Nm) | 0.636 | 1.318 | 1.715 | 2.073 | 2.285 |
| $T_{avg}$ for Hybrid E-core SRM (Nm) | 0.480 | 1.302 | 1.851 | 2.382 | 2.655 |

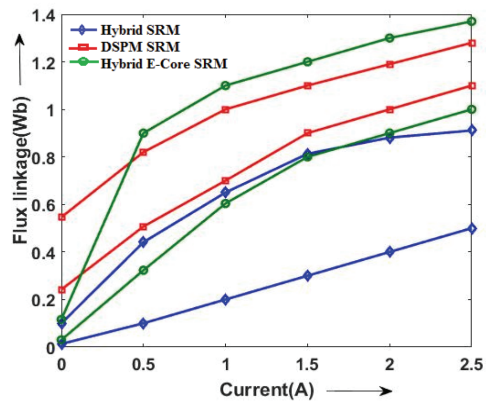


Fig. 12. Comparison of phase flux linkage characteristics for the three different configurations of SRM.

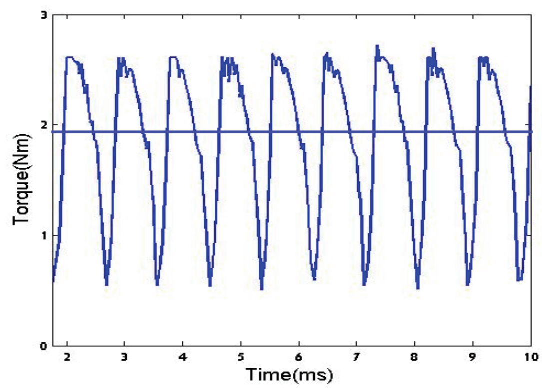


Fig. 13. Dynamic torque characteristics of Hybrid SRM at rated current.

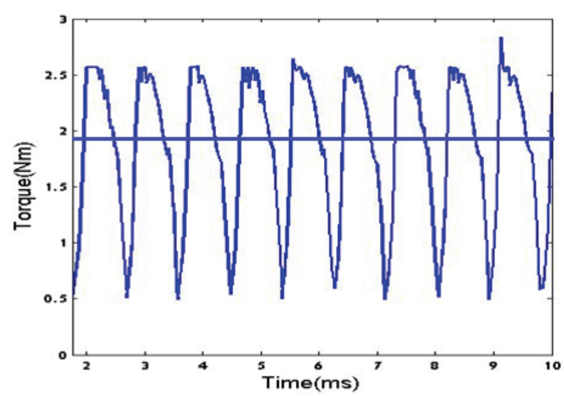


Fig. 14. Dynamic torque characteristics of DSPM SRM at rated current.

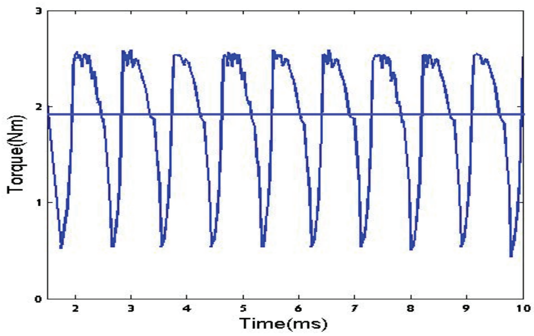


Fig. 15. Dynamic torque characteristics of Hybrid E-core SRM at rated current.

TABLE IV
COMPARISON OF PERFORMANCE PARAMETERS

| Parameters | Hybrid SRM | DSPM SRM | Hybrid E-core SRM |
|---|---|---|---|
| Torque ripple (%) | 52.4 | 42.5 | 50.6 |
| Cogging Torque (Nm) | 0.001 | 0.28 | 0.001 |
| Conductive loss (W) | 62.2 | 53 | 44 |
| Iron Loss (W) | 22.57 | 10.37 | 20 |
| Total losses (W) | 84.77 | 63.37 | 64 |

The dynamic torque characteristics for all the three different configurations of SRM are shown in Fig. 13, 14 and 15.

To highlight the superior performance of proposed hybrid E-core structure of SRM over DSPM SRM and hybrid SRM, a comparison is drawn with respect to losses, efficiency, torque ripple and cogging torque and are presented in Table IV. Torque ripple is obtained from [22].

$$T_{ripple} = (T_{max}-T_{min})/T_{max} \quad (3)$$

Where $T_{max}$ is the peak of static torque profile, which is called the maximum torque and $T_{min}$ is the torque at the intersection instants. From Table IV it is clear that torque ripple value of hybrid E-core SRM is nearly 8% higher than DSPM SRM however it is 2% lower than hybrid SRM. The conductive loss of hybrid E-core SRM is less than DSPM SRM and hybrid SRM. The cogging torque value of hybrid E-core configuration is very low when compared with DSPM configuration of SRM. Moreover, proposed hybrid E-core SRM configuration employs cheaper ferrite magnets, while DSPM SRM employs NdFeB magnets which also results in cost saving.

## IV. VIBRATION ANALYSIS

The most important shortcoming of SRM for industrial and domestic applications is its acoustic noise [23]. Studies from literature reveal that radial force acting on the stator and torque ripple are the major sources of vibration in SRM, whose magnitude depends on switching techniques and frequency. Hence, for designing a low noise SRM it is essential to determine the frequencies at which radial forces are induced in stator core, since the coincidence of stator's natural frequency with any of the modal frequency will cause resonance thereby resulting in vibration [25]. The modal analysis is performed to determine the natural frequency of vibration. The detailed flow diagram for performing vibration analysis is illustrated in Fig. 16.

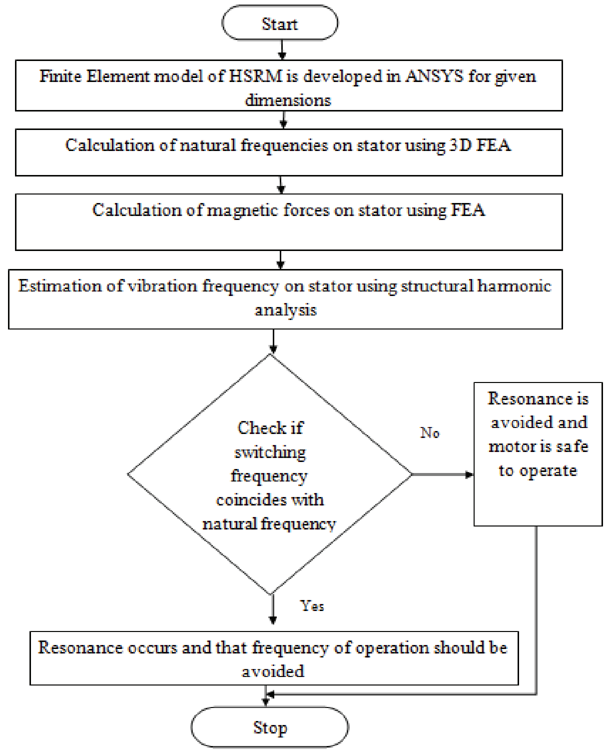


Fig. 16. Flow chart for vibration analysis.

The equation of vibration for the under damped condition is given by equation (4) [26]

$$[M]y''(t) + [K]y'(t) = 0 \quad (4)$$

Where, y(t) is the mode displacement vector

[M] is the mass matrix;

[K] is the stiffness matrix.

The free vibration solution will be harmonic and of the form:

$$\{y(t)\} = e^{\omega jt}\{\varphi\}_j \quad (5)$$

Where, $\{\varphi\}_j$ is the eigen vector representing the mode shapes of the $j^{th}$ natural frequency and $\omega_j$ is the $j^{th}$ mode frequency. This equation leads to eigen problem and to get modal frequency equation (5) should be solved using modal analysis.

In ANSYS environment the FEA model of hybrid E-core SRM is developed. The Young's modulus, Poisson's ratio and mass density properties have been properly chosen for stator steel, copper coil and ferrite magnet areas. The mode shapes obtained from 3-D analysis of hybrid E-core SRM and their corresponding displacement magnitudes along with their natural frequencies are depicted in Fig. 17. It can be inferred from Fig. 17 that mode 4 has the maximum displacement and mode 2 has the least.

Using the same procedure shown in Fig. 16, the first five natural frequencies of vibration are determined for three

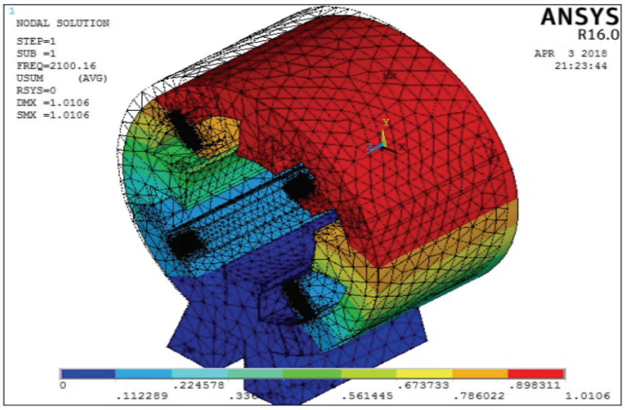


(a)

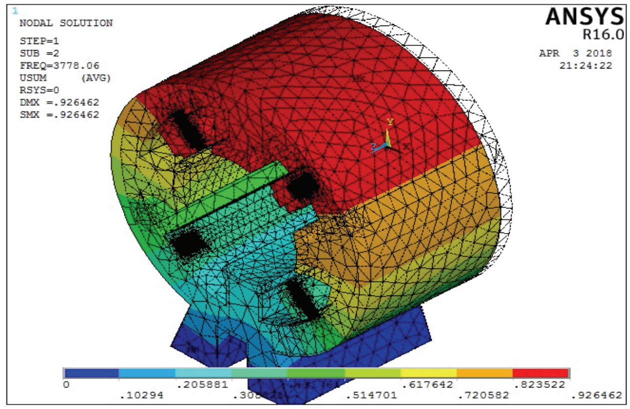


(b)

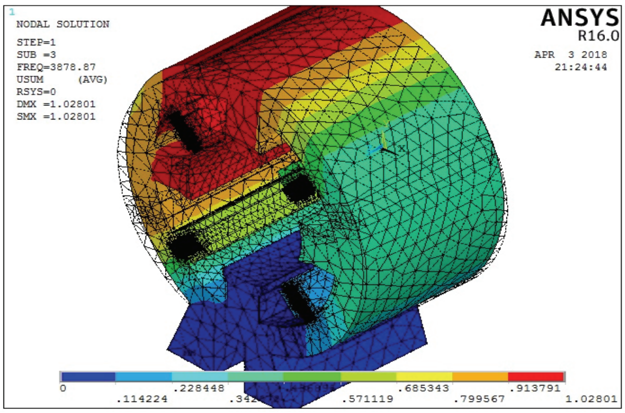


(c)

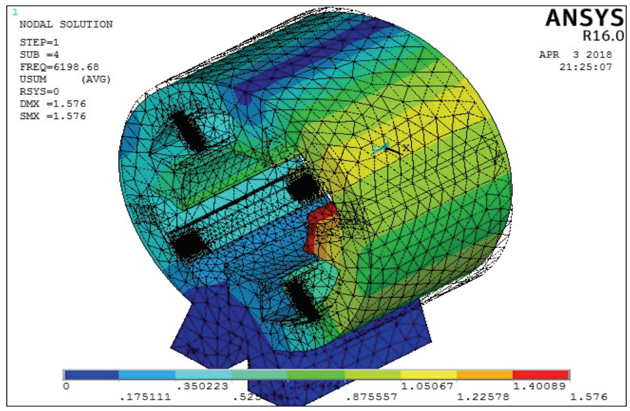


(d)

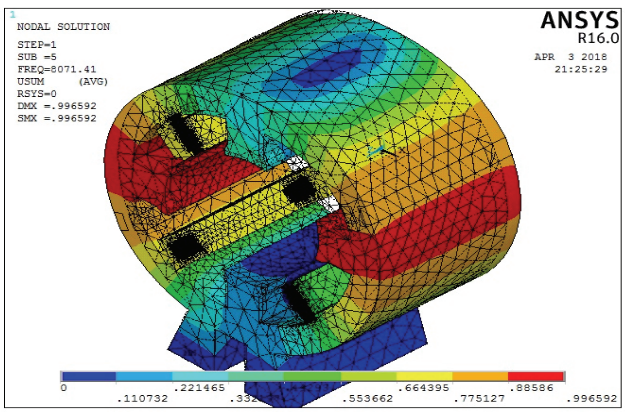


(e)

Fig. 17. Stator mode shapes of hybrid E-core SRM using 3-D FEA. (a) Mode 1(2100 Hz). (b) Mode 2 (3778 Hz). (c) Mode 3 (3878 Hz). (d) Mode 4 (6198 Hz). (e) Mode 5 (8071 Hz).

TABLE V
NATURAL FREQUENCIES FOR THREE DIFFERENT CONFIGURATIONS OF SRM

| Mode | Hybrid E-core SRM | DSPM SRM | Hybrid SRM |
|---|---|---|---|
| 1 | 2100 Hz | 1538Hz | 2269Hz |
| 2 | 3778Hz | 3058Hz | 4003Hz |
| 3 | 3878Hz | 3248Hz | 4863Hz |
| 4 | 6198Hz | 5818Hz | 6664Hz |
| 5 | 8071Hz | 6854Hz | 8474Hz |

configurations of SRM and are listed in Table V. From Table V it is evident that hybrid SRM operates at higher natural frequency. To predict the stator vibration frequencies and their magnitudes, harmonic structural analysis is performed. The normal and tangential force components are estimated by performing electromagnetic FEA using MagNet. The calculated force is then applied to the stator surface and harmonic structural analysis is carried out for predicting the displacement in X and Y direction for all the three configurations of SRM. The displacement in X and Y direction for Hybrid E-core SRM

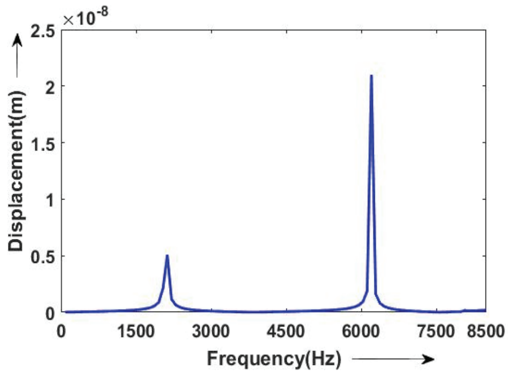


Fig. 18. X direction displacement vs frequency due to normal and tangential forces for hybrid E-core SRM.

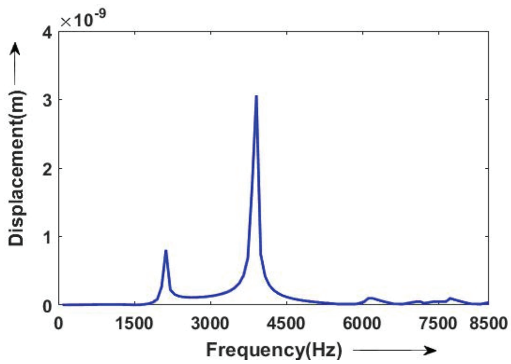


Fig. 19. Y direction displacement vs frequency due to normal and tangential forces for hybrid E-core SRM.

TABLE VI
COMPARISON OF DISPLACEMENT VALUES

| Configuration | Displacement(m) | |
|---|---|---|
| | X direction | Y direction |
| Hybrid E-core SRM | $2.2X\ 10^{-8}$ | $3X\ 10^{-9}$ |
| DSPM SRM | $3.2X\ 10^{-8}$ | $3X\ 10^{-8}$ |
| Hybrid SRM | $0.52\ X\ 10^{-8}$ | $0.83\ X\ 10^{-8}$ |

obtained from harmonic analysis is shown in Fig. 18 and Fig. 19. The magnitudes of vibration for all the three configurations of SRM are tabulated in Table VI.

From the results of harmonic analysis given in Table VI, it is evident that the magnitude of vibration is less in hybrid SRM along X direction and in hybrid E-core SRM along Y direction. In hybrid E-core SRM the displacement value in X direction is higher at 6100Hz (nearer to fourth mode) and at 3900Hz (nearer to third mode) in Y direction as shown in Fig. 18 and Fig. 19. In order to avoid resonance the hybrid E-core SRM should not be operated at 6100Hz and 3900Hz.

## V. CONCLUSION

This paper presents the performance analysis of a hybrid E-core SRM with auxiliary windings and permanent magnets in stator yoke. The electromagnetic and vibration characteristics of this proposed configuration are compared with the existing DSPM SRM and hybrid SRM. From the analysis and comparative study the following conclusions can be drawn.

a) The hybrid E-core SRM has better flux linkage vs current characteristics and produces higher value of average torque in comparison with DSPM SRM and hybrid SRM.
b) The torque ripple value of hybrid E-core SRM is 8% higher than that of DSPM SRM and 2% lesser than that of hybrid SRM.
c) On comparing the losses it is evident that the conductive loss of hybrid E-core SRM is less than that of DSPM SRM and hybrid SRM.
d) The hybrid E-core SRM and hybrid SRM have very low values of cogging torque in comparison with DSPM SRM.
e) The hybrid E-core SRM outperforms DSPM SRM with respect to the natural frequencies of vibration and the magnitude of displacement

Thus, it can be concluded that the proposed hybrid E-core configuration of SRM has better performance characteristics. The future work will be oriented towards torque ripple minimization and controller design for hybrid E-core configuration of SRM.


## ACKNOWLEDGMENT

This research has been supported by Department of Science and Technology, Ministry of Science and Technology, Government of India under the Fast track Young Scientist- Engineering Science Scheme (SB/FTP/ETA-0189/2014/17. 07.2015).


## REFERENCES


[1] H. Cheng, H. Chen, S. Xu, and S. Yang, "Adaptive variable angle control in Switched Reluctance Motor Drives for Electric Vehicle applications," *J. Power Electron.*, Vol. 17, No. 6, pp. 1512-1522, Nov. 2017.

[2] H. Zeng, Z. Chen, and H. Chen, "Smooth torque speed characteristics of switched reluctance motor," *J. Power Electron.*, Vol. 14, No. 2, pp. 341-350, Mar. 2014.

[3] G. Bhuvaneswari, S. G. Thakurta, P. S. Rao, and S. S. Murthy, "Modeling of switched reluctance motor in sensorless and with sensor modes," *J. Power Electron.*, Vol. 6, No. 4, pp. 315-321, Oct. 2006.

[4] Y. Liao, F. Liang, and T. A. Lipo, "A novel Permanent Magnet motor with Doubly salient structure," *IEEE Trans. Ind. Appl.*, Vol. 31, No. 5, pp. 1069-1078, Sep. 1995.

[5] S.-H. Mao and M.-C. Tsai, "A novel switched reluctance motor with C core stator," *IEEE Trans. Magn.,*Vol. 41, No.12, pp:4413~4420,Dec. 2005.

[6] S.-G. Oh and R. Krishnan, "Two-phase SRM with flux-reversal-free stator: concept, analysis, design, and experimental verification," *IEEE Trans. Ind. Appl.,* Vol. 43, No.5, pp. 1247-1257, Oct. 2007.

[7] C. Lee, R. Krishnan, and N. S. Lobo, "Novel two-phase switched reluctance machine using common-pole e-core structure: Concept, analysis, and experimental verification,"

*IEEE Trans. Ind. Electron.*, Vol. 45, No. 2, pp. 703-711, Apr. 2009.

[8] T. H. Kim, "A study on the design of an inset-permanent-magnet-type flux-reversal machine," *IEEE Trans. Magn.,* Vol. 45, No. 6, pp. 2859-2862, Jun. 2009.

[9] K. Lu, U. Jakobsen, and P. O. Rasmussen, "Single-phase hybrid switched reluctance motor for low-power low-cost applications," *IEEE Trans. Magn*., Vol. 47, No. 10, pp. 3288-3291, Oct. 2011.

[10] Y. Hasegawa, K. Nakamura, and O. Ichinokura, "A novel switched reluctance motor with the auxiliary windings and permanent magnets," *IEEE Trans. Magn.,* Vol. 48, No. 11, pp. 3855-3858, Nov. 2012.

[11] H. Eskandari and M. Mirsalim, "An improved 9/12 two-phase E-core switched reluctance machine," *IEEE Trans. Energy. Convers.,* Vol. 28, No. 4, pp. 951-958, Dec. 2013.

[12] D. Wu, J. T. Shi, Z. Q. Zhu, and X. Liu, "Electromagnetic performance of novel synchronous machines with permanent magnets in stator yoke," *IEEE Trans. Magn.,* Vol. 50, No. 9, Sep. 2014.

[13] L. Xu, W. Zhao, J. Ji, G. Liu, Y. Du, Z. Fang, and L. Mo, "Design and analysis of a new linear hybrid excited flux reversal motor with inset permanent magnets," *IEEE Trans. Magn.,* Vol. 50, No. 11, Nov. 2014.

[14] H. Zhang, D.-H. lee, C.-W. Lee, and J.-w. Ahn, "design and analysis of segmented rotor type 12/8 switched reluctance motor," *J. Power Electron.*, Vol. 14, No. 5, pp. 866-872, Oct. 2014.

[15] W. Hua, P. Su, M. Tong, and J. Meng, "Investigation of a five-phase E-core hybrid-excitation flux-switching machine for EV and HEV applications," *IEEE Trans. Ind. Appl*., Vol. 55, No. 1, pp. 124-133, Jan. 2017.

[16] Z.-C. You, S.-M. Yang, C.-W. Yu, Y.-H. Lee, and S.-C. Yang, "Design of a high starting torque single-phase DC-excited flux switching machine," *IEEE Trans. Ind. Elect*., Vol. 64, No. 12, pp. 9905-9913, Dec. 2017.

[17] P. Su, W. Hua, Z. Wu, P. Han, and M. Cheng, "Analysis of the operation principle for rotor-permanent-magnet flux-switching machines," *IEEE Trans. Ind. Electron.,* Vol. 65, No. 2, pp. 1062-1073, Feb. 2018.

[18] C. Lee, "Analysis and design of novel e-core common pole switched reluctance machine," PhD thesis, Virginia Polytechnic Institute and State University, Mar. 2010.

[19] M. Masoumi and M. Mirsalim, "E-core hybrid reluctance motor with permanent magnets inside common stator poles," *IEEE Trans. Energy Conv.,* Vol. 33, No. 2, pp. 826-833, Jun. 2018.

[20] R. Krishnan, Switched Reluctance Motor Drives Modelling, Simulation, Analysis, Design and Applications, Boca Rotan, CRC Press, 2001.

[21] N. S. Lobo, "Doubly-salient permanent magnet flux-reversal-free-stator switched reluctance machines," PhD thesis, Virginia Polytechnic Institute and State University, Jan. 2011

[22] F. Sahin, H. B. Ertan, and K. Leblebicioglu, "Optimum geometry for torque ripple minimization of switched reluctance motors," *IEEE Trans. Energy Convers.*, Vol. 15, No. 1, pp. 30-39, Mar. 2000.

[23] W. Cai, P. Pillay, Z. Tang, and A. M. Omekanda, "Low-vibration design of switched reluctance motors for automotive applications using modal analysis," *IEEE Trans. Ind. Appl.,* Vol. 39, No. 4, pp. 971-977, Aug. 2003.

[24] J.-H. Lee, Y.-H. Lee, D.-H. Kim, K.-S. Lee, and I.-H. Park, "Dynamic vibration analysis of switched reluctance motor using magnetic charge force density and mechanical analysis," *IEEE Trans. Appl. Supercond.,* Vol. 12, No. 1, pp. 1511-1514, Mar. 2002.

[25] K. N. Srinivas and R. Arumugam, "Static and dynamic vibration analyses of switched reluctance motors including bearings, housing, rotor dynamics, and applied loads," *IEEE Trans. Magn*., Vol. 40, No. 4, pp. 1911-1919, Jul. 2004.

[26] P. Pillay and W. Cai, "An investigation into vibration in Switched reluctance Motors," *IEEE Trans. Ind. Appl.,* Vol. 32, No. 4, pp. 589-596, May 1999.

**Saranya S.** was born in India, 1988. She received her B. E Degree in Electronics and Communication Engineering from Bharathidasan University, Tiruchirapalli, India in 2010, M.E Degree in Power Electronics and Drives from Anna University, Chennai, India in 2012 and presently working towards her PhD degree. Her current research interest includes electrical machines and drives.

**Balaji M.** was born in 1980 in India. He received his B. E Degree in Electrical and Electronics Engineering from Annamalai University, Chidambaram, India in 2002, M.E Degree in Power Electronics & Drives from Anna University, Chennai, India in 2004 and Ph.D degree from Anna University in 2012. He is presently working as an Associate Professor in the Department of Electrical and Electronics Engineering, SSN College of Engineering, Kalavakkam, India. His current research interest includes electrical machines and drives.